Desalination and Water Treatment
www.deswater.com

doi: 10.5004/dwt.2021.27757

238 (2021) 142–150
October

Frictional interpretation of Peusner resistance coefficients of the polymeric membranes for binary solutions of non-electrolytes

Andrzej Ślęzak[a], Jolanta Jasik-Ślęzak[b], Kornelia M. Batko[c], Wioletta M. Bajdur[b], Maria Włodarczyk-Makuła[d,*]

[a]*Department of Health Science, Jan Dlugosz University, 13/15 Armia Krajowa Al. 42200 Częstochowa, Poland, email: aslezak52@gmail.com*
[b]*Faculty of Management, Częstochowa University of Technology, 35b Armia Krajowa Al. 42200 Częstochowa, Poland, emails: jolantajasik-slezak@wz.pcz.pl (J. Jasik-Ślęzak)*
[c]*Department of Business Informatics, University of Economics in Katowice, 2B Bogucicka, 40287 Katowice, Poland, email: kornelia.batko@ue.katowice.pl*
[d]*Department of Enviromental Engineering, Częstochowa University of Technology, 69 Dabrowskiego Str., 42200 Częstochowa, Poland, email: mwm@is.pcz.pl*

Received 1 August 2021; Accepted 25 August 2021

ABSTRACT

The *R* version of the Kedem–Katchalsky–Peusner (KKP) network equations belongs to the group of basic research tools for membrane transport. These equations contain the Peusner resistance coefficients (R_{ij}, R_{det}) used to assess the transport properties of membranes. The aim of the paper was the frictional interpretation of these coefficients for binary solutions of non-electrolytes on the basis of the Spiegler model. The subject of the study was the transport properties of synthetic polymer membranes made of regenerated cellulose and used in hemodialysis (Nephrophan, Ultra-Flo 145 Dialyzer) for aqueous glucose solutions. The research method was the *R* version of the KKP network equations and the Kedem–Katchalsky–Spiegler equation for binary solutions of non-electrolytes. The method of frictional interpretation of the Peusner resistance, coupling, Kedem–Caplan–Peusner energy conversion efficiency and dissipated and free energy fluxes using the Spiegler friction coefficients (f_{ij}) was presented. The presented procedure for evaluation transport properties of membranes can be helpful in explaining the mechanisms of membrane transport and conducting energy analyzes of membrane processes. Therefore, this procedure can be used for the selection of a suitable membrane for practical, (e.g., industrial, water and wastewater technology and/or medical) applications.

Keywords: Membrane transport; Kedem–Katchalsky–Peusner equations; Spiegler model; Synthetic polymeric membrane; Energy conversion; Water technology

1. Introduction

Water with appropriate biological and physicochemical parameters is an essential component of the intracellular environment, ensuring the proper course of life processes [1]. The cell membrane, which has built-in switches that respond to environmental signals and transmit information to intracellular protein pathways, plays a key role in the process of responding to environmental signals [2]. This means that the quality and length of life depend on the quality of food and water consumed.

Membrane transport is one of the basic natural phenomena. It occurs in both natural and artificial physicochemical systems. For this reason, it plays an important

* Corresponding author.

role in life processes and therefore is present in science, biomedicine and technology [1]. Artificial (polymeric) membranes play an important role as separators in systems such as hemodialyzers, active membrane dressings, installations for sewage treatment or food production [1,3]. The assessment of the suitability of polymer membranes as separators is usually based on membrane transport models developed within the framework of near-equilibrium thermodynamics proposed by Onsager [4] (linear non-equilibrium thermodynamics, LNET) and network thermodynamics (NT).

Onsager [4] thermodynamics deals with the phenomenology of interacting processes (chemical, electrical, etc.). Considering the generalized thermodynamic forces X_i and the coupled J_i fluxes that occur in the bilinear dissipation function.

$$\Phi_S = \frac{T}{A}\frac{d_i S}{dt} = \frac{1}{A}\sum_{i=1}^{n} J_i X_i \tag{1}$$

where Φ_S is the dissipation function (W m^2); $d_i S/dt$ is the entropy production (W K^{-1}); T is the temperature (K); A is the surface area (m^2).

Onsager's theory establishes that irreversible coupling between various processes can occur if $\Phi_S > 0$. If the X_i and J_i are related by linear equations of the form $X_i = \sum_{k=1}^{n} R_{ik} J_k$, the coefficient matrix R is symmetric ($R_{ik} = R_{ki}$). In addition, Onsager thermodynamics dealt with the extreme properties of energy, entropy, and the dissipation function [4–7].

According to the principles of Onsager thermodynamics, they were deduced by Kedem and Katchalsky [8] and Hoshoko and Lindley [9] sets of equations describing passive and active membrane transport of water and solutes. The procedure for deriving these sets of equations requires finding the Φ_S and transforming it to account for appropriate practical forces and fluxes to obtain macroscopic phenomenological equations [10].

Passive membrane transport of non-electrolyte through membrane generated by hydrostatic (ΔP) and osmotic ($\Delta\pi$) pressures can be described by Kedem–Katchalsky equations. The equations have the form [5,8]:

$$J_v = L_p\left(\Delta P - \sigma\Delta\pi\right) \tag{2}$$

$$J_s = \omega\Delta\pi + \overline{C}_s\left(1-\sigma\right)J_v \tag{3}$$

where J_v is the volume flux (m s^{-1}); J_s is the solute flux (mol m^{-2} s^{-1}); ΔP is the difference of hydrostatic pressure (Pa); $\Delta\pi$ is the difference of osmotic pressure (Pa); L_p is the hydraulic permeability coefficient (m^3 N^{-1} s^{-1}); σ is the reflection coefficient; ω is the solute permeability coefficient (mol N^{-1} s^{-1}); $\overline{C}_s$ is the average solute concentration (mol m^{-3}).

The flux of degraded energy, that is, the energy dissipation function (Φ_S) can be described by the equation [5]:

$$\Phi_S = J_v\left(\Delta P - \Delta\pi\right) + J_s\frac{\Delta\pi}{\overline{C}} \tag{4}$$

In the 1960s, there were attempts to formulate the principles of network thermodynamics, based on Meixner's [11] pioneering ideas on the relationship between irreversible transport systems and electrical networks. There are two versions of NT in science: Peusner NT [12] and Oster et al. NT [13]. The idea of network thermodynamics, based on the linear thermodynamics of irreversible processes and the theory of electric circuits, was introduced by Leonardo Peusner (Peusner's network thermodynamics, PNT) in the 1970s [12]. In subsequent papers [14–18], Peusner developed this idea, among others, for energy conversion systems [14–16], membrane systems and processes [15,16], Brownian motion [17] and biochemical reactions [18]. In [14–16] Peusner presented methods of symmetric and hybrid transformation of network linear Onsager equations and classical Kedem–Katchalsky equations. Four forms of these equations (L, R, H, P) for homogeneous binary solutions contain the Peusner tensor coefficients L_{ij}, R_{ij}, H_{ij} and P_{ij} ($i, j \in \{1,2\}$) [14–16]. Network thermodynamics extended Onsager's ideas, formally showing that the macroscopic structure of non-equilibrium thermodynamics is homologous to the family of lattices that obey Kirchhoff's laws [14].

The papers of Peusner were an inspiration for the development of symmetrical and hybrid transformations of the network Kedem–Katchalsky (KK) equations, KK equations for the conditions of concentration polarization and the introduction of Peusner tensor coefficients L_{ij}^z, R_{ij}^z, H_{ij}^z and P_{ij}^z, ($i, j \in \{1,2\}$, $z = A, B$) [19–24]. We have shown that the values of these coefficients depend on both the concentration and composition of the solutions separated by the membrane. They also depend on the orientation of the membrane and solutions in relation to the gravity vector, that is, the configuration of the membrane system.

In the paper by Batko et al. [25], the coupling coefficients (r_{ij}) ($i, j \in \{1,2\}$), the energy conversion efficiencies $(e_{ij})_R$ and the coupling coefficients Q_R were defined and calculated, using the concentration relationships of the coefficients $R_{ij} = f\left(\overline{C}\right)$ and $R_{\text{det}} = f\left(\overline{C}\right)$ for bioprocess, Nephrophan and Ultra-Flo 145 Dialyzer membranes and aqueous glucose solutions. Moreover, the concentration characteristics of the dissipation function $(\Phi_S)_R$ and the concentration characteristics of the free energy production function $(\Phi_F)_R$ were calculated.

The aim of the present paper is to further develop the Kedem–Katchalsky–Peusner model: frictional interpretation of the Peusner coefficients R_{ij} and R_{det} ($i, j \in \{1,2\}$) for aqueous glucose solutions. Appropriate calculations of these factors for Nephrophan and Ultra-Flo 145 Dialyzer made of polymeric materials used in medicine biomembranes were performed. The concentration characteristics of the Peusner (R_{11}, R_{12}, R_{21}, R_{22}, R_{det}), coupling coefficients (r_{12}, r_{21}, Q_R) and energy conversion efficiency coefficient $(e_{\max})_R$ were calculated on the basis of the transport parameters: hydraulic permeability (L_p), reflection (σ) and solute permeability (ω). The values of parameters L_p, σ and ω were determined in a series of independent experiments for aqueous glucose solutions and membranes Nephrophan, Ultra-Flo 145 Dialyzer according to the procedure described in [5]. Moreover, the frictional version of the Peusners coefficients R_{ij} and R_{det} ($i, j \in \{1,2\}$) was presented. The internal energy conversion by determining

the degraded (*S*-energy), free (*F*-energy) and internal energy (*U*-energy) fluxes were described. The presented considerations can be used to describe the membrane separation in the water and wastewater, technology.

2. Materials and methods

2.1. Peusner model of transport in the membrane cell

As in the previous paper by Batko et al. [25], we will consider a single-membrane system, the model of which is presented in Fig. 1. In this system, the membrane (*M*) separates two homogeneous solutions with C_r and C_l concentrations ($C_r \geq C_l$) and hydrostatic pressures P_r and P_l ($P_r > P_l$, $P_r = P_l$ or $P_r < P_l$). This membrane treated as a "black box" type is isotropic, symmetrical, electroneutral and selective for solvent and dissolved substance. We will consider only isothermal and stationary processes of membrane transport, for which the measure is the volume (J_v) and solute (J_s) fluxes. The membrane transport properties were characterized by the coefficients: hydraulic permeability (L_p), reflection (σ) and solute permeability (ω).

Relationships between the volume (J_v) and solute (J_s) fluxes and the osmotic pressure ($\Delta\pi$) and hydrostatic pressure (ΔP) differences can be expressed using the *R* form of the Kedem–Katchalsky–Peusner equations [16,22,25].

$$\begin{bmatrix} \Delta P - \Delta\pi \\ \dfrac{\Delta\pi}{\overline{C}} \end{bmatrix} = \left[R\right] \begin{bmatrix} J_v \\ J_s \end{bmatrix} \tag{5}$$

$$\left[R\right] = \begin{bmatrix} R_{11} & R_{12} \\ R_{21} & R_{22} \end{bmatrix} = \begin{bmatrix} \dfrac{\omega + L_p \overline{C}_s \left(1-\sigma\right)^2}{L_p \omega} & -\dfrac{1-\sigma}{\omega} \\ -\dfrac{1-\sigma}{\omega} & \dfrac{1}{\overline{C}_s \omega} \end{bmatrix} \tag{6}$$

where J_v is the volume flux (m s^{-1}); J_s is the solute flux (mol m^{-2} s^{-1}); $\Delta P = P_r - P_l$ is the difference of hydrostatic pressure (Pa); $\Delta\pi = RT(C_r - C_l)$ is the difference of osmotic pressure (Pa); RT is the product of a gas constant and absolute temperature (J mol^{-1}); C_r, C_l is the solute concentrations (mol m^{-3}) L_p is the hydraulic permeability coefficient (m^3 N^{-1} s^{-1}); σ is the reflection coefficient; ω is the solute permeability coefficient (mol N^{-1} s^{-1}); $\overline{C}_s = \left(C_r - C_l\right)\left[\ln\left(C_r / C_l\right)\right]^{-1}$ is the average solute concentration (mol m^{-3}); R_{11} is the Peusner's hydraulic resistance (Ns m^{-3}); R_{12}, R_{21} ($R_{12} = R_{21}$) is the Peusner's coupling resistance (Ns mol^{-1}); R_{22} is the Peusner's diffusion resistance (m^3 Ns mol^{-2}).

Eqs. (5) and (6) are obtained by transforming Eqs. (2) and (3). In addition, the determinant of the matrix [*R*] is given by the equation:

$$\det\left[R\right] = \frac{1}{L_p \overline{C}_s \omega} \equiv R_{\text{det}} \tag{7}$$

The coefficients R_{ij} ($i, j \in \{1,2\}$) and R_{det} are the *R* form of the Peusner coefficients for membrane transport of binary solutions.

2.2. Frictional form of Peusner coefficients

The coefficients R_{ij} ($i, j \in \{1,2\}$) and R_{det}, written by Eqs. (5) and (6), can be expressed by the coefficients f_{ij}, whose frictional character of intermolecular interactions is illustrated by the expression [26].

$$F_{kj} = -f_{kj}\left(v_k - v_j\right) \tag{8}$$

where F_{kj} is the frictional force (N mol^{-1}), f_{kj} is the coefficient of friction between one mole of the *k*-th and one mole of the *j*-th component (Ns mol^{-1} m^{-1}), v_k and v_j are the velocities of the *k*-th and *j*-th components, respectively (m s^{-1}).

The friction model was developed by Kurt Samuel Spiegler, one of the pioneers in the research and development of liquid desalination technology, including water [27]. Hence with Eq. (8) we can write $F_{\text{sw}} = -f_{\text{sw}}(v_s - v_w)$, $F_{\text{sm}} = -f_{\text{sm}}(v_s - v_m)$ and $F_{\text{wm}} = -f_{\text{wm}}(v_w - v_m)$ [28,29]. Choosing the membrane as the frame of reference it follows that $v_m = 0$. Detailed considerations on the friction model and its developments are presented in [28–31]. For the purposes of this paper, we cite expressions that transform the coefficients L_p, σ and ω into friction coefficients f_{kj}, assuming that there are three types of friction between the solute and water in the membrane: the frictional interaction of the solute with its surrounding solvent characterized by coefficient f_{sw}; the friction of solute with the membrane described by f_{sm}; and that of water and membrane given by coefficient f_{wm}. In the paper [29] it was shown that for binary solutions of non-electrolyte solutions there are dependencies between the coefficients L_p, σ, ω, f_{sw}, f_{sm}, and f_{wm}.

$$L_p = \frac{\varphi_w \overline{V}_w}{\Delta x f_{\text{wm}}} \tag{9}$$

$$1 - \sigma = \frac{K_s\left(\overline{V}_w f_{\text{sw}} + \overline{V}_s f_{\text{wm}}\right)}{\varphi_w \overline{V}_w \left(f_{\text{sw}} + f_{\text{sm}}\right)} \tag{10}$$

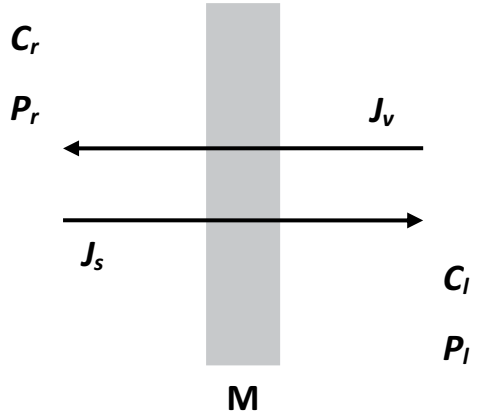

Fig. 1. The single-membrane system: *M* – membrane, J_v – volume flux, J_s – solute flux, C_r and C_l – concentrations of solute separated by a membrane, P_r and P_l – hydrostatic pressures [25].

$$\omega = \frac{K_s}{\Delta x\left(f_{sw} + f_{sm}\right)} \tag{11}$$

Taking into account Eqs. (9)–(11) in Eqs. (5) and (6) we get:

$$R_{11} = \frac{\Delta x\left[f_{wm}\varphi_w \bar{V}_w\left(f_{sw} + f_{sm}\right) + \bar{C}_s K_s\left(\bar{V}_w f_{sw} + \bar{V}_s f_{wm}\right)^2\right]}{\varphi_w^2 \bar{V}_w^2\left(f_{sw} + f_{sm}\right)} \tag{12}$$

$$R_{12} = R_{21} = -\frac{\Delta x\left(\bar{V}_w f_{sw} + \bar{V}_s f_{wm}\right)}{\varphi_w \bar{V}_w} \tag{13}$$

$$R_{22} = \frac{\Delta x\left(f_{sw} + f_{sm}\right)}{\bar{C}_s K_s} \tag{14}$$

$$R_{det} = \frac{\Delta x^2 f_{wm}\left(f_{sw} + f_{sm}\right)}{\varphi_w \bar{V}_w K_s \bar{C}_s} \tag{15}$$

where $\varphi_w = \bar{V}_w \bar{C}_w$, K_s is the distribution coefficient, $\bar{V}_w$ and $\bar{V}_s$ are the partial molar volume for water (index w) and solute (index s) (m^3 mol^{-1}), Δx is the thickness of the membrane (m).

In order to show the relationship between coefficients R_{12}, R_{21}, R_{11} and R_{22} we will calculate the Kedem–Caplan degree coupling $r_{12} = R_{12} / \sqrt{R_{11}R_{22}}$ and $r_{21} = R_{12} / \sqrt{R_{11}R_{22}}$ using Eqs. (12)–(14). The expressions for these coefficients take the following forms:

$$r_{12} = r_{21} = \left(\bar{V}_w f_{sw} + \bar{V}_s f_{wm}\right) \sqrt{\frac{\bar{C}_s K_s}{f_{wm}\varphi_w \bar{V}_w\left(f_{sw} + f_{sm}\right) + \bar{C}_s K_s\left(\bar{V}_w f_{sw} + \bar{V}_s f_{sm}\right)^2}} \tag{16}$$

The values of r_{12} and r_{21} coefficients are limited by the relation $-1 \le r_{12}, r_{21} \le +1$. In order to show the relationship between coefficients r_{12} and r_{21} we will calculate the Peusner coupling parameter $Q_R = r_{12}r_{21}/(2-r_{12}r_{21})^{-1}$ using Eq. (16):

$$Q_R = \frac{\bar{C}_s K_s\left(\bar{V}_w f_{sw} + \bar{V}_s f_{sm}\right)^2}{2 f_{wm}\varphi_w \bar{V}_w\left(f_{sw} + f_{sm}\right) + \bar{C}_s K_s\left(\bar{V}_w f_{sw} + \bar{V}_s f_{sm}\right)^2} \tag{17}$$

2.3. Evaluation of internal energy conversion

The internal energy conversion process is governed by the principle of conservation of energy. According to this principle, the flux of the internal energy (Φ_U), free energy (Φ_F) and degraded (dissipated) energy (Φ_S) flux satisfy the equation [25].

$$\Phi_U = \Phi_F + \Phi_S \tag{18}$$

where $\Phi_U = A^{-1}dU/dt$ is the internal energy flux (U-energy) (W m^{-2}), $\Phi_F = A^{-1}dF/dt$ is the free energy flux (F-energy) (W m^{-2}), $\Phi_S = TA^{-1}\, d_i S/dt$ is the degraded energy flux (energy dissipation function per unit area) (S-energy) (W m^{-2}) and $\Phi_S = T\varphi_S$, φ_S is the entropy production (W K^{-1}).

The flux of degraded energy, that is, the energy dissipation function (Φ_S) can be described using Eq. (4) [5]. In order to calculate J_v and J_s appearing in Eq. (4), we use Eqs. (5) and (6). By making appropriate transformations, we get:

$$\left(J_v\right)_R = \frac{R_{22}}{R_{11}R_{22} - R_{12}R_{21}}\left[\Delta P - \left(\bar{C}_s + \frac{R_{12}}{R_{22}}\right)\frac{\Delta\pi}{\bar{C}_s}\right] \tag{19}$$

$$\left(J_s\right)_R = \frac{R_{11}}{R_{11}R_{22} - R_{12}R_{21}}\left[\left(1 + \frac{R_{21}}{R_{22}}\bar{C}_s\right)\frac{\Delta\pi}{\bar{C}_s} - \frac{R_{21}}{R_{11}}\Delta P\right] \tag{20}$$

where

$$\frac{R_{22}}{R_{11}R_{22} - R_{12}R_{21}} = \frac{f_{sw} + f_{sm}}{\Delta x f_{wm}\varphi_w}$$

$$\frac{R_{11}}{R_{11}R_{22} - R_{12}R_{21}} = \frac{f_{wm}\varphi_w\left(f_{sw} + f_{sm}\right) + \bar{C}_s K_s\left(\bar{V}_w f_{sw} + \bar{V}_s f_{wm}\right)^2}{\Delta x f_{wm}\varphi_w\left(f_{sw} + f_{sm}\right)^2}$$

$$\frac{R_{12}}{R_{22}} = \frac{R_{21}}{R_{22}} = -\frac{\bar{C}_s K_s}{\varphi_w \bar{V}_w}\frac{\bar{V}_w f_{sw} + \bar{V}_s f_{wm}}{f_{sw} + f_{sm}}$$

$$\frac{R_{12}}{R_{11}} = \frac{R_{21}}{R_{11}} = -\frac{\left(\bar{V}_w f_{sw} + \bar{V}_s f_{wm}\right)\left(f_{sw} + f_{sm}\right)\varphi_w^2 \bar{V}_w^2}{f_{wm}\varphi_w\left(f_{sw} + f_{sm}\right) + \bar{C}_s K_s\left(\bar{C}_s K_s\right)^2}$$

Taking into account Eqs. (19) and (20) in Eq. (4) we get:

$$\left(\Phi_S\right)_R = \boldsymbol{\mathcal{R}}\begin{bmatrix} R_{22}\left(\Delta P\right)^2 + \left(\alpha_1 + \alpha_2\right)\left(\frac{\Delta\pi}{\bar{C}_s}\right)^2 \\ -\left(R_{22}\bar{C}_s + R_{21} + \alpha_3\right)\frac{\Delta\pi}{\bar{C}_s}\Delta P \end{bmatrix} \tag{21}$$

where

$$\boldsymbol{\mathcal{R}} = \left(R_{11}R_{22} - R_{12}R_{21}\right)^{-1} = \left(\varphi_w \bar{V}_w^2 \bar{C}_s K_s\right)\left[\Delta x^2 f_{wm}\left(f_{sw} + f_{sm}\right)\right]^{-1},$$

$$\alpha_1 = R_{22}\bar{C}_s\left(\bar{C}_s + \frac{R_{12}}{R_{22}}\right),\ \alpha_2 = R_{11}\left(1 + \frac{R_{12}}{R_{22}}\bar{C}_s\right),\ \alpha_3 = R_{22}\left(\bar{C}_s + \frac{R_{12}}{R_{22}}\right)$$

For $\Delta P = 0$, the above equation is simplified to the form:

$$\left(\Phi_S\right)_R = \frac{\Delta\pi^2}{R_{11}R_{22} - R_{12}R_{21}}\left[R_{22}\left(1 + \frac{R_{12}}{\bar{C}_s R_{22}}\right) + \frac{R_{11}}{\bar{C}_s^2}\left(1 + \frac{\bar{C}_s R_{21}}{R_{11}}\right)\right] \tag{22}$$

The free energy flux $(\Phi_F)_R$ can be calculated using the definition of the energy conversion efficiency coefficient [25].

$$\left(e_{max}\right)_R = \frac{\left(\Phi_F\right)_R}{\left(\Phi_U\right)_R} = \frac{\left(\Phi_F\right)_R}{\left(\Phi_F\right)_R + \left(\Phi_S\right)_R} \tag{23}$$

By transforming the above expression, we get:

$$\left(\Phi_F\right)_R = \frac{\left(e_{max}\right)_R}{1 - \left(e_{max}\right)_R}\left(\Phi_S\right)_R \tag{24}$$

$$\left(\Phi_U\right)_R = \frac{1}{1-\left(e_{\max}\right)_R}\left(\Phi_S\right)_R \tag{25}$$

From a formal point of view, the cases of $(\Phi_F)_R = 0$ and $(\Phi_U)_R = 0$ are excluded, because in order for the denominator of Eqs. (24) and (25) to be different from zero, the condition $(e_{max})_R \neq 1$ must be satisfied.

In Eqs. (24) and (25) $(e_{max})_R$ is the maximum energy conversion efficiency expressed by the Kedem–Caplan–Peusner coefficient [6,7,14], which can be represented as follows.

$$\left(e_{\max}\right)_R = \frac{R_{12}R_{21}}{R_{11}R_{22}\left(1+\sqrt{1-\frac{R_{12}R_{21}}{R_{11}R_{22}}}\right)^2} = \frac{r_{12}r_{21}}{\left(1+\sqrt{1-r_{12}r_{21}}\right)^2} \tag{26}$$

The values of $(e_{max})_R$ coefficient are limited by the relation $0 \le (e_{max})_R \le 1$; $(e_{max})_R = 0$ when $R_{12}R_{21} = 0$ or $r_{12}r_{21} = 0$ and $(e_{max})_R = 1$, when $R_{12}R_{21} = R_{11}R_{22}$ or $r_{12}r_{21} = 1$.

3. Results and discussion

3.1. Biomembranes characteristics

Images of Nephrophan and Ultra-Flo 145 Dialyzer membranes obtained with a scanning electron microscope (Zeiss Supra 35) were shown in a previous paper [25]. Suitable values of the transport parameters (L_p, σ, ω) and friction coefficients (f_{wm}, f_{sw}, f_{sm}) of these membranes are listed in Table 1. Nephrophan® (ORWO VEB Filmfabrik, Wolfen, Germany) biomembrane, is a microporous, highly hydrophilic and electroneutral membrane made of regenerated cellulose [32]. This membrane is used in urology in ganglion hemodialyzers for the purification of venous blood. Ultra-Flo 145 Dialyzer® (Artificial Organs Division, Travenol Laboratories, Brussels, Belgium) (with regenerated cellulose membrane) is ultrafiltration, microporous, hydrophilic and electroneutral biomembrane used in urology [3].

Table 1
Values of the transport parameters (L_p, σ, ω) and friction coefficients (f_{wm}, f_{sw}, f_{sm}) of Nephrophan and Ultra-Flo 145 Dialyzer biomembranes for aqueous glucose solution

Coefficient	Value	
	Nephrophan	Ultra-Flo 145 Dialyzer
$L_p \times 10^{12}$ ($m^3\ N^{-1}\ s^{-1}$)	4.9	2.7
$\sigma \times 10^2$	6.8	8.3
$\omega \times 10^{10}$ ($mol\ N^{-1}\ s^{-1}$)	8.0	7.1
$\Delta x \times 10^4$ (m)	2.0	0.8
φ_w	0.71	0.68
K_s	0.53	0.6
$\bar{V}_w \times 10^6$ ($m^3\ mol^{-1}$)	18.05	18.05
$\bar{V}_s \times 10^6$ ($m^3\ mol^{-1}$)	120.2	120.2
$f_{wm} \times 10^{-10}$ ($Ns\ mol^{-1}\ m^{-1}$)	1.31	5.68
$f_{sw} \times 10^{-10}$ ($Ns\ mol^{-1}\ m^{-1}$)	111.32	867.47
$f_{sm} \times 10^{-10}$ ($Ns\ mol^{-1}\ m^{-1}$)	220.13	696.98

The frictional form of the coefficients R_{ij} ($i, j \in \{1,2\}$) and R_{det} for an aqueous solution of glucose were calculated on the basis of Eqs. (8)–(11). The transport parameters (L_p, σ, ω) and the friction coefficients (f_{wm}, f_{sw}, f_{sm}) of the Nephrophan and Ultra-Flo 145 Dialyzer membranes presented in Table 1 were used for the calculations. Calculations were made concerning the dependence of coefficients R_{ij} ($i, j \in \{1,2\}$) and R_{det} from $\bar{C}_s$. Fig. 2a–d shows the dependence of R_{11}, $R_{12} = R_{21}$, R_{22} and R_{det} on the glucose concentration ($\bar{C}_s$) for Nephrophan (plots 1) and Ultra-Flo 145 Dialyzer (plots 2) membranes.

Based on Eqs. (9)–(11) and the values of the coefficients L_p, σ and ω calculated the friction coefficients (f_{wm}, f_{sw}, f_{sm}) for Nephrophan and Ultra-Flo 145 membranes. The values of these coefficients for urea are presented in Table 1.

3.2. Calculations of Peusner coefficients R_{ij} and R_{det}

The frictional form of the coefficients R_{ij} ($i, j \in \{1,2\}$) and R_{det} for an aqueous solution of urea were calculated on the basis of Eqs. (12)–(15). The transport parameters (L_p, σ, ω) and the friction coefficients (f_{wm}, f_{sw}, f_{sm}) of the Nephrophan, Ultra-Flo 145 Dialyzer and red blood cell membranes presented in Table 1 were used for the calculations. Fig. 2a–d shows the dependence of R_{11}, $R_{12} = R_{21}$, R_{22} and R_{det} on the glucose concentration ($\bar{C}_s$) for Nephrophan (plots 1), Ultra-Flo 145 Dialyzer (plots 2) membranes.

Graphs 1 and 2 shown in Fig. 2a show that the dependencies $R_{11} = f\left(\bar{C}_s\right)$ are linear and that for the same values of $\bar{C}_s$ the values of R_{11} for the red blood cells membrane are greater than for the Ultra-Flo 145 Dialyzer membrane and for the membrane Nephrophan. Graphs 1 and 2 presented in Fig. 2a show that the values R_{11} are limited by the relations $2.48 \times 10^{11}\ Ns\ m^{-3} \le R_{11} \le 5.45 \times 10^{11}\ Ns\ m^{-3}$ (for the Nephrophan membrane) and $4.27 \times 10^{11}\ Ns\ m^{-3} \le R_{11} \le 8.08 \times 10^{11}\ Ns\ m^{-3}$ (for the Ultra-Flo 145 Dialyzer membrane). Plots 1 and 2 shown in Fig. 2b show that $R_{12} = R_{21}$ are negative and independent of $\bar{C}_s$ and that the values of $R_{12} = R_{21}$ for the Nephrophan membrane and is greater than for the Ultra-Flo 145 Dialyzer membrane. For the membrane Nephrophan $R_{12} = R_{21} = -0.34 \times 10^9\ Ns\ mol^{-1}$ and for the membrane Ultra-Flo 145 Dialyzer $R_{12} = R_{21} = -1.06 \times 10^9\ Ns\ mol^{-1}$.

Plots 1–3 shown in Fig. 2c show that the dependencies $R_{22} = f\left(\bar{C}_s\right)$ are hyperbolas and that for the same values of $\bar{C}_s$ the values of R_{22} for the Ultra-Flo 145 Dialyzer membrane and is greater than for the Nephrophan membrane. Graphs 1 and 2 presented in Fig. 2c show that the values R_{22} are limited by the relations $4.48 \times 10^8\ m^3\ Ns\ mol^{-2} \ge R_{22} \ge 0.57 \times 10^8\ m^3\ Ns\ mol^{-3}$ (for the Nephrophan membrane) and $7.48 \times 10^8\ m^3\ Ns\ mol^{-2} \ge R_{22} \ge 0.96 \times 10^8\ m^3\ Ns\ mol^{-2}$ (for the Ultra-Flo 145 Dialyzer membrane). Similarly, plots 1 and 2 shown in Fig. 2d show that the dependencies $R_{det} = f\left(\bar{C}_s\right)$ are hyperbolas and that for the same values of $\bar{C}_s$ the values of R_{det} for the Ultra-Flo 145 Dialyzer membrane and is greater than for the Nephrophan membrane. Graphs 1 and 2 presented in Fig. 2d show that the values R_{det} are limited by the relations $9.15 \times 10^{19}\ N^2\ s^2\ mol^{-2} \ge R_{det} \ge 1.18 \times 10^{19}\ N^2\ s^2\ mol^{-2}$ (for the Nephrophan membrane) and $27.68 \times 10^{19}\ N^2\ s^2\ mol^{-2} \ge R_{det} \ge 3.56 \times 10^{19}\ N^2\ s^2\ mol^{-2}$ (for the Ultra-Flo 145 Dialyzer membrane).

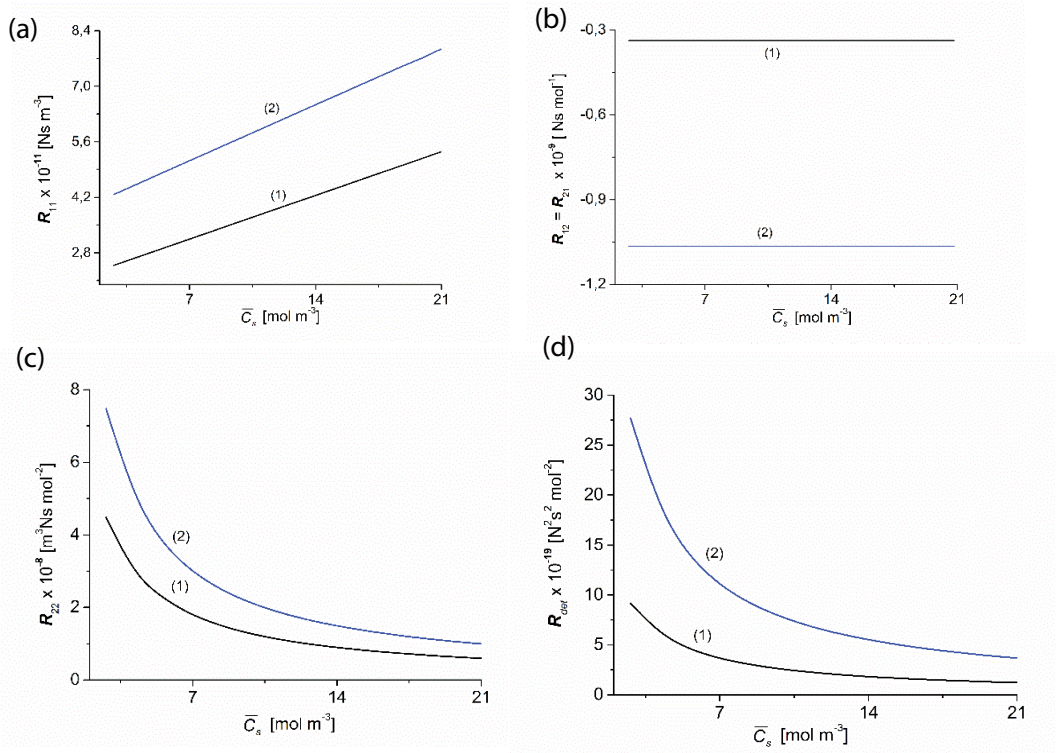

Fig. 2. Graphical illustration of dependencies of $R_{11} = f\left(\bar{C}_s\right)$ (a), $R_{12} = R_{21} = f\left(\bar{C}_s\right)$ (b), $R_{22} = f\left(\bar{C}_s\right)$ (c) and $R_{\text{det}} = f\left(\bar{C}_s\right)$ (d) for Nephrophan (Graphs 1) and Ultra-Flo 145 Dialyzer membranes (Graphs 2).

The coefficients R_{ij} ($i, j \in \{1,2\}$) and R_{det} are called Peusner resistance coefficients. Taking into account Eqs. (5) and (6), it is possible to define the coefficients R_{11}, R_{12}, R_{21} and R_{22} using the expressions:

$$R_{11} = \left(\frac{\Delta P - \Delta\pi}{J_v}\right)_{J_s=0} \tag{27}$$

$$R_{12} = \left(\frac{\Delta P - \Delta\pi}{J_s}\right)_{J_v=0} = \left(\frac{\Delta\pi_s}{\bar{C}_s J_v}\right)_{J_s=0} = R_{21} \tag{28}$$

$$R_{22} = \left(\frac{\Delta\pi_s}{\bar{C}_s J_s}\right)_{J_v=0} \tag{29}$$

The physical sense of these coefficients is different as their units are different. The unit of the coefficient R_{11} is Ns m^{-3}. Therefore, these coefficients express the hydraulic resistance. The unit of the coefficients $R_{12} = R_{21}$ is Ns mol^{-1}. The unit of the R_{22} coefficient is Ns m^3 mol^{-2}. This coefficient expresses the diffusion resistance per unit of the average molar concentration of the solution. In turn, the unit of the R_{det} coefficient is N^2 s^2 mol^{-2}. This means that this coefficient expresses the square of the diffusion resistance.

3.3. Calculations of coefficients r_{12} and Q_R

Taking into account the values of the coefficients listed in Table 1 in Eqs. (16) and (17), the dependencies $r_{12} = r_{21} = f\left(\bar{C}_s\right)$ and $Q_R = f\left(\bar{C}_s\right)$ were calculated. The calculation results are shown in curves 1 and 2 in Fig. 3a and b. These figures show that the dependencies $r_{12} = r_{21} = f\left(\bar{C}_s\right)$ and $Q_R = f\left(\bar{C}_s\right)$ are nonlinear and that for the same values of $\bar{C}_s$ both $r_{12} = r_{21}$ and Q_R for the Nephrophan membrane are smaller than for the Ultra-Flo 145 Dialyzer membrane. Graphs 1 and 2 presented in Fig. 3a show that the values $r_{12} = r_{21}$ are limited by the relations $0.011 \le r_{12} = r_{21} \le 0.019$ (for the Nephrophan membrane) and $0.019 \le r_{12} = r_{21} \le 0.038$ (for the Ultra-Flo 145 Dialyzer membrane). On the other hand, Graphs 1 and 2 presented in Fig. 3b show that the Q_R values are limited by the relations $5.2 \times 10^{-5} \le Q_R \le 1.86 \times 10^{-4}$ (for the Nephrophan membrane) and $1.75 \times 10^{-4} \le Q_R \le 7.2 \times 10^{-4}$ (for the Ultra-Flo 145 Dialyzer membrane).

3.4. Calculations of energy conversion efficiency $(e_{max})_R$

Taking into account the values of the Peusner coefficients R_{11}, R_{12} and R_{22} presented in Fig. 2a–c in Eq. (26), the dependencies $\left(e_{\max}\right)_R = f\left(\bar{C}_s\right)$ were calculated. The calculation results are shown in curves 1, 2 and 3 in Fig. 4a. These figures show that the dependencies $\left(e_{\max}\right)_R = f\left(\bar{C}_s\right)$ are linear and that for the same values of $\bar{C}_s$ both $(e_{\max})_R$ for the Nephrophan membrane are greater than for the Ultra-Flo 145 Dialyzer membrane and red blood cell membranes. Graphs 1–3 presented in Fig. 4a show that the values $(e_{\max})_R$ are limited by the relations $0.26 \times 10^{-3} \le (e_{\max})_R \le 0.93 \times 10^{-3}$ (for the Nephrophan membrane) and $0.87 \times 10^{-3} \le (e_{\max})_R \le 3.61 \times 10^{-3}$ (for the Ultra-Flo 145 Dialyzer membrane).

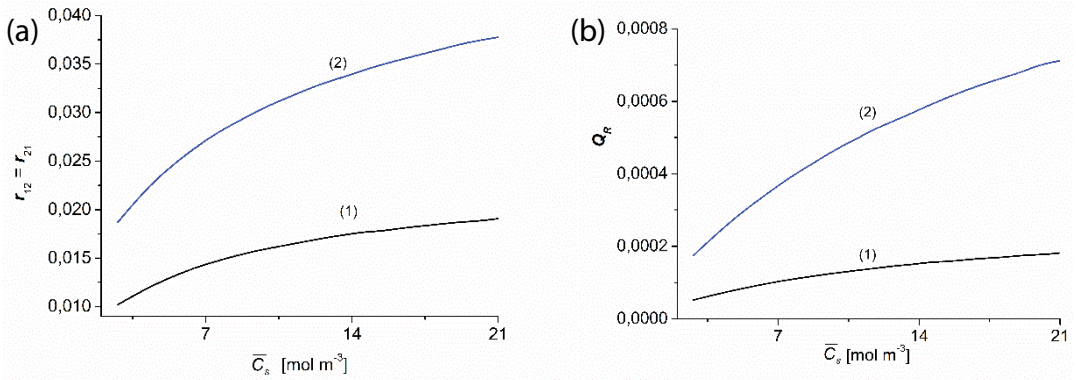

Fig. 3. Graphical illustration of dependencies of $r_{12} = r_{21} = f\left(\overline{C}_s\right)$ (a) and $Q_R = f\left(\overline{C}_s\right)$ (b) for Nephrophan (Graphs 1) and Ultra-Flo 145 Dialyzer membranes (Graphs 2).

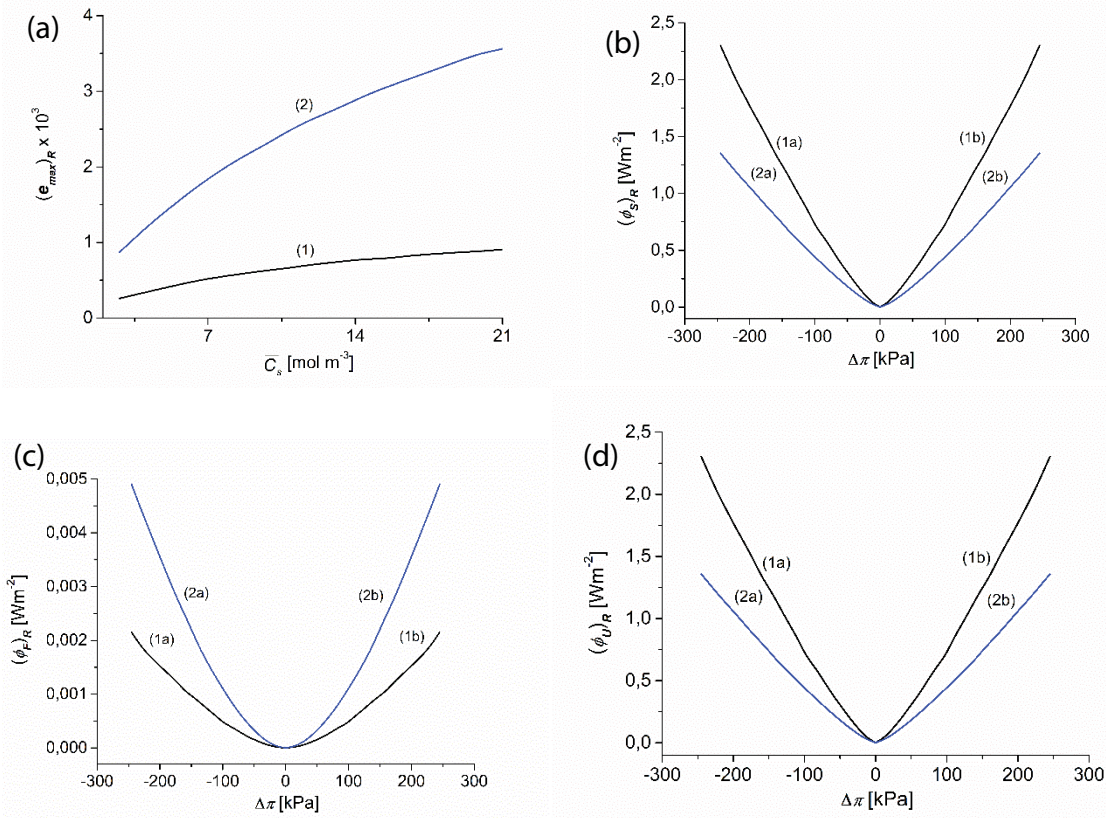

Fig. 4. Graphical illustration of dependencies of $\left(e_{\max}\right)_R = f\left(\overline{C}_s\right)$ (a), $(\Phi_S)_R = f(\Delta\pi)$ (b), $(\Phi_F)_R = f(\Delta\pi)$ (c) and $(\Phi_U)_R = f(\Delta\pi)$ (d) for Nephrophan (Graphs 1) and Ultra-Flo 145 Dialyzer membranes (Graphs 2).

3.5. Evaluation of the internal energy conversion

Conversion of internal energy (*U*-energy) is its transformation into free energy (*F*-energy) and degraded energy (*S*-energy). The *S*-energy denoted by $(\Phi_S)_R$ can be expressed using Eq. (21). This equation includes the Peusner coefficients R_{ij} (i, $j \in \{1,2\}$) and the thermodynamic stimuli ΔP and $\Delta\pi$. The calculations of $(\Phi_S)_R = f(\Delta\pi)$ were made for the case of $\Delta P = 0$ (Eq. 22) and the results of the calculations are presented in Fig. 4b. All the characteristics of this are isosceles parabolas. The figure shows that for the same $\Delta\pi$ values, the $(\Phi_S)_R$ values for the Nephrophan membrane (plots 1a, 1b) are greater than for the Ultra-Flo 145 Dialyzer membrane (plots 2a, 2b). Graphs 1 and 2 presented in Fig. 4b show that the values $(\Phi_S)_R$ are limited by the relations 0.041 W m^{-2} ≤ $(\Phi_S)_R$ ≤ 2.3 W m^{-2} (for the Nephrophan membrane) and 0.026 W m^{-2} ≤ $(\Phi_S)_R$ ≤ 1.35 W m^{-2} (for the Ultra-Flo 145 Dialyzer membrane).

Fig. 4c shows the results of the calculations $(\Phi_F)_R$ in the form of characteristics $(\Phi_F)_R = f(\Delta\pi)$ calculated on the basis of the Eq. (23) for the characteristics $\left(e_{\max}\right)_R = f\left(\overline{C}_s\right)$ and $(\Phi_S)_R = f(\Delta\pi)$, presented in Fig. 4a and b, respectively. The

characteristics presented in Fig. 4c are isosceles parabolas. The figure shows that for the same $\Delta\pi$ values, the $(\Phi_F)_R$ values obtained for the Ultra-Flo 145 Dialyzer membrane (plots 2a, 2b) are greater than for the Nephrophan membrane (plots 1a, 1b). Graphs 1–3 presented in Fig. 4b show that the values $(\Phi_F)_R$ are limited by the relations $0 \le (\Phi_F)_R \le 0.0021$ W m^{-2} (for the Nephrophan membrane) and $0 \le (\Phi_F)_R \le 0.0049$ W m^{-2} (for the Ultra-Flo 145 Dialyzer membrane).

Fig. 4d shows the results of the calculations $(\Phi_U)_R$ in the form of the characteristics $(\Phi_U)_R = f(\Delta\pi)$ calculated on the basis of Eq. (25) for the characteristics $\left(e_{\max}\right)_R = f\left(\overline{C}_s\right)$ and $(\Phi_S)_R = f(\Delta\pi)$, presented in Fig. 4a and b, respectively. The characteristics presented in Fig. 4d are isosceles parabolas. The figure shows that for the same $\Delta\pi$ values, the highest $(\Phi_U)_R$ values obtained for the Nephrophan membrane (plots 1a, 1b) are greater than for the Ultra-Flo 145 Dialyzer membrane (plots 2a, 2b). Graphs 1 and 2 presented in Fig. 4b show that the values $(\Phi_U)_R$ are limited by the relations 0.041 W m^{-2} $\le (\Phi_U)_R \le$ 2.303 W m^{-2} (for the Nephrophan membrane) and 0.026 W m^{-2} $\le (\Phi_U)_R \le$ 1.36 W m^{-2} (for the Ultra-Flo 145 Dialyzer membrane).

4. Conclusions

- The aim of the paper was the frictional interpretation of these coefficients for binary solutions of non-electrolytes on the basis of the Spiegler model.
- The values of the f_{sw}, f_{sm} and f_{wm} coefficients for Nephrophan and Ultra-Flo 145 Dialyzer membranes do not depend on glucose concentrations.
- The method of frictional interpretation of the Peusner resistance (R_{ij}; $i, j \in \{1,2\}$, R_{det}), coupling degree ($r_{12} = r_{21}$ and Q_R), Kedem–Caplan–Peusner energy conversion efficiency ($(e_{\max})_R$) and dissipated ($(\Phi_S)_R$), free ($(\Phi_F)_R$) and internal ($(\Phi_U)_R$) energy fluxes using the Spiegler friction coefficients (f_{ij}) was presented.
- The glucose concentration characteristics of the Peusner resistance (R_{ij}; $i, j \in \{1,2\}$, R_{det}), coupling degree ($r_{12} = r_{21}$ and Q_R), Kedem–Caplan–Peusner energy conversion efficiency ($(e_{\max})_R$) and dissipated ($(\Phi_S)_R$), free ($(\Phi_F)_R$) and internal ($(\Phi_U)_R$) energy fluxes.
- The frictional form of the R_{ij} ($i, j \in \{1,2\}$) and R_{det} coefficients may be helpful in explaining the molecular mechanisms of membrane transport in both biological and artificial systems.
- The tested membranes are poor internal energy converters, because the amount produced by the *F*-energy does not exceed 5 mW m^{-2}.
- The presented procedure for evaluating the transport properties of membranes can be helpful in explaining the mechanisms of membrane transport and conducting energy analyzes of membrane processes. Therefore, this procedure can be used for the selection of a suitable membrane for practical, (e.g., industrial, water and wastewater technology or medical) applications.

References

[1] R. Baker, Membrane Technology and Application, John Wiley & Sons, New York, 2012.

[2] B.H. Lipton, S. Bhaerman, Spontaneous Evolution – Our Positive Future and a Way to Get There From Here, Hay House Inc., USA, 2009.

[3] Z.J. Twardowski, History of hemodialyzers' designs, Hemodialysis Int., 12 (2008) 173–210.

[4] L. Onsager, Reciprocal relations in irreversible processes. I., Phys. Rev., 37 (1931) 405–426.

[5] A. Katchalsky, P.F. Curran, Non-equilibrium Thermodynamics in Biophysics, Harvard University Press, Cambridge,1965.

[6] O. Kedem, S.R. Caplan, Degree of coupling and its relation to efficiency of energy conversion, Trans. Faraday Soc., 61 (1965) 1897–1911.

[7] S.R. Caplani, The degree of coupling and its relation to efficiency of energy conversion in multiple-flow systems, J. Theor. Biol., 10 (1965) 209–235.

[8] O. Kedem, A. Katchalsky, Permeability of composite membranes. Part 1.–Electric current, volume flow and flow of solute through membrane, Trans. Faraday Soc., 59 (1961) 1918–1930.

[9] T. Hoshoko, B.D. Lindley, Phenomenological description of active transport of salt and water, J. Gener. Physiol., 50 (1967) 729–758.

[10] L. Peusner, Hierarchies of irreversible energy conversion systems. II. Why are Onsager equations? The Euclidean geometry of fluctuation–dissipation space, J. Theor. Biol., 122 (1986) 125–155.

[11] J. Meixner, Thermodynamics of electrical networks and the Onsager–Casimir reciprocal relation, J. Math. Phys., 4 (1963) 154–159.

[12] L. Peusner, The Principles of Network Thermodynamics: Theory and Biophysical Applications, Ph.D. Thesis, Harvard University, Cambridge, Massachusetts, 1970.

[13] G. Oster, A. Perelson, A. Katchalsky, Network thermodynamics, Nature, 234 (1971) 393–399.

[14] L. Peusner, Studies in Network Thermodynamics, Elsevier, Amsterdam, 1986.

[15] L. Peusner, Hierarchies of irreversible energy conversion systems: a network thermodynamics approach. I. Linear steady state without storage, J. Theor. Biol., 10 (1983) 27–39.

[16] L. Peusner, Hierarchies of irreversible energy conversion systems. II. Network derivation of linear transport equations, J. Theor. Biol., 115 (1985) 319–335.

[17] L. Peusner, Network representation yelding the evolution of Brownian motion with multiple particle interactions, Phys. Rev., 32 (1985) 1237–1238.

[18] L. Peusner, A network thermodynamic approach to Hill and King-Altman reaction-diffusion kinetics, J. Chem. Phys., 83 (1985) 5559–5566.

[19] K.M. Batko, I. Ślęzak-Prochazka, S. Grzegorczyn, A. Ślęzak, Membrane transport in concentration polarization conditions: network thermodynamics model equations, J. Porous Media, 17 (2014) 573–586.

[20] K.M. Batko, I. Ślęzak-Prochazka, A. Ślęzak, Network hybrid form of the Kedem–Katchalsky equations for non-homogenous binary non-electrolyte solutions: evaluation of P^*_{ij} Peusner's tensor coefficients, Trans. Porous Media, 106 (2015) 1–20.

[21] I. Ślęzak-Prochazka, K.M. Batko, S. Wąsik, A. Ślęzak, H^* Peusner's form of the Kedem–Katchalsky equations for non-homogeneous non-electrolyte binary solutions, Trans. Porous Media, 111 (2016) 457–477.

[22] A. Ślęzak, S. Grzegorczyn, K.M. Batko, Resistance coefficients of polymer membrane with concentration polarization, Trans. Porous Media, 95 (2012) 151–170.

[23] A. Ślęzak, S. Grzegorczyn, K.M. Batko, W.M. Bajdur, M. Włodarczyk-Makuła, Applicability of the L^r form of the Kedem–Katchalsky–Peusner equations for membranę transport in water purification technology, Desal. Water Treat., 202 (2020) 48–60.

[24] K.M. Batko, A. Ślęzak, S. Grzegorczyn, W.M. Bajdur, The R^r form of the Kedem–Katchalsky–Peusner model equations for description of the membranę transport in concentration polarization conditions, Entropy, 22 (2020) 857 (1–27), doi: 10.3390/e22080857.

[25] K.M. Batko, A. Ślęzak, W. Pilis, Evaluation of transport properties of biomembranes by means of Peusner network thermodynamics, Acta Bioeng. Biomech., 2 (2021) 63–72.
[26] K.S. Spiegler, Transport process in ionic membranes, Trans. Faraday Soc., 54 (1958) 1408–1428.
[27] K.S. Spiegler, O. Kedem, Thermodynamics of hyperfiltration (reverse osmosis): criteria for efficient membranes, Desalination, 1 (1966) 311–326.
[28] O. Kedem, A. Katchalsky, A physical interpretation of the phenomenological coefficients of membrane permeabilty, J. Gen. Physiol., 45 (1961) 143–179.
[29] A. Ślęzak, A frictional interpretation of the phenomenological coefficients of the membranę permeability for mlticomponent non-ionic solutions, J. Biol. Phys., 23 (1997) 239–250.
[30] A. Ślęzak, B. Turczyński, Generalization of the Spiegler–Kedem–Katchalsky frictional model equations of the transmembrane transport for multicomponent non-electrolyte solutions, Biophys. Chem., 44 (1992) 139–142.
[31] A. Ślęzak, S. Grzegorczyn, J. Wąsik, Model equations for interactions of hydrated species transmembrane transport, Desalination, 163 (2004) 177–192.
[32] H. Klinkman, M. Holtz, W. Willgerodt, G. Wilke, D. Schoenfelder, Nephrophan – eine neue dialysemembran, Zeitschrift für Urologie, 4 (1969) 285–292.